

Dynamical controls on estuarine bathymetry: assessment against UK data base

David Prandle*

Proudman Oceanographic Laboratory, Joseph Proudman Building, 6 Brownlow Street, Liverpool L3 5DA, UK

Abstract

New theories for estuarine bathymetry provide formulations for: i) depth at the mouth, D versus river flow, Q ; ii) tidal intrusion length L versus D and Z (tidal amplitude) and iii) a zone of morphological existence, delineated on a framework of Z versus D . Here, these theories are assessed against a database for 80 UK estuaries. Overall there is good agreement between theory and observations for the sizes and shapes of estuaries classified as either ‘Coastal Plain’ or ‘Bar Built’. Likewise, most estuaries are shown to lie within the theoretical ‘zone of bathymetric existence’.

These encouraging agreements enable the theories to be used to: i) enhance our understanding of existing morphologies, ii) identify anomalous estuaries and iii) make future predictions regarding likely impacts from global climate change and related management scenarios. Subsequent examination of regional historical patterns of morphological evolution, introducing detailed local knowledge, should help to explain these anomalies and refine the new theories.

By 2100, we anticipate changes in UK estuaries due to (‘precautionary’) projected 25% changes in river flow of: Order (0.5 to 5 km) in lengths and Order (50 to 250 m) in breadths. Corresponding changes due to a projected sea level rise of 50 cm are: increases in both lengths of Order (1 to 2.5 km) and breadths of Order (70 to 100 m). In both cases, the bigger changes will occur in larger estuaries.

Keywords: bathymetry, morphology, tides, salinity, climate change, UK

1. Introduction

Lane (2004) examined the bathymetric evolution of the Mersey Estuary over the twentieth century. Lane and Prandle (2006) demonstrated uncertainties associated with attempts to reproduce these changes via numerical model simulations. In many countries, commercial

* E-mail: davidprandle@hotmail.co.uk (D. Prandle)

exploitation of estuaries is restricted by this lack of confidence in the use of such models for predicting long-term bathymetric evolution. To circumvent this, attempts have been made to develop ‘Hybrid’ models – combining the dynamical rigour of numerical models alongside the observational experience encapsulated in rule-based geomorphological models (Woodroffe, 2003).

Prandle (2004a) sought to derive rule-based morphological expressions by simplification of the one-dimensional equation of axial momentum propagation. Resulting theories provide explicit formulations for: i) depth at the mouth, D , as a function of river flow, Q , ii) tidal intrusion length L as $f(D, Z)$, where Z is the tidal elevation amplitude at the mouth and iii) a bounded zone of likely estuarine morphologies defined by Z and D . (D is a ‘representative’ maximum depth at the mouth and L stretches from the mouth to the upstream limit of tidal elevation changes for mean tidal and river flow conditions). Further details of the development of these theories are presented in Section 2.

Paradoxically, these morphological expressions take no account of the prevailing sediment regime resulting in a paradigm shift suggesting that the sediment regime is a consequence rather than a determinant of morphology! Prandle (2004b) investigated this conclusion, indicating what sediment could co-exist with these morphologies, i.e., yield no net deposition or accretion. The results provided new insights into how estuaries selectively trap and axially sort sediments. Prandle et al. (2005) show that these indicated sediment regimes are broadly consistent with observations in a number of European estuaries.

A recently available morphological data set (Future-Coast, Burgess et al., 2002) for 80 estuaries in England and Wales provided an opportunity to assess the validity of these radical new theories. Here we present this assessment. To separate results for differing geomorphological types in this assessment, we use the same classifications as Davidson and Buck (1997). While the results overall are encouraging, many anomalies and wide scatter between observed and theoretical bathymetries are shown. Possible explanations for this scatter and ways of reducing this by more selective applications are described in Section 5.

Section 2 summarises the new dynamically-based theories relating to estuarine bathymetries. Section 3 describes the systematic derivation from the published data sets of representative estuarine parameters: D , Z , Q , breadth B and side-slope ‘ a ’. UK estuaries

include large inter-tidal zones, with breadths at high tide typically three or more times low tide values. Hence in both the theoretical developments and in the analyses of observed morphologies triangular cross sections were assumed with side-slope $a = 2D/B$.

Section 4 inter-compares these theories and observations. In Section 4.1, mean values of the above parameters are calculated for three differing estuarine morphological types, namely Rias, Coastal Plain and Bar Built. In addition minimum values of both D and Q required for estuarine functioning are examined. Section 4.2 analyses the relationships between the morphological parameters D , B and L . In Section 4.3, the relationships of the latter with the ‘forcing’ parameters Z and Q are examined.

Section 5 summarises results and conclusions and illustrates forecasts of estuarine morphologies for the year 2100 for various Global Climate Change scenarios.

2. Theory

Prandle (2003) sought to derive rule-based morphological expressions by simplification of the one-dimensional equation of axial momentum propagation. Use was made of the ‘synchronous’ assumption, i.e. where axial gradients related to tidal phase (in either elevation or current) predominate over gradients in amplitude. This yields explicit expressions for tidal current amplitude U_T and bed slope $\partial D/\partial x$ terms in terms of tidal elevation amplitude Z and depth D .

2.1 Tidal length, L

Integration of the expression for $\partial D/\partial x$ yields both an estimate of overall tidal propagation length, L and an axial profile of depth, Equations (1) and (2) respectively.

$$L = 123 D^{5/4} / (Z^{1/2} f^{1/2}) = 2460 D^{5/4} / Z^{1/2} \quad (\text{m}), \quad (1)$$

where the bed friction coefficient f is assumed to be 0.0025. This result is shown in Figure 1 alongside conditions for sandy estuaries where a doubling of ‘ f ’ reduces L by a factor $2^{1/2}$ and for muddy estuaries where the converse applies. Section 4.2 indicates that this ‘synchronous’ assumption is likely to be applicable for all but the longest of UK estuaries.

2.2 Shape

The above theory indicates an axial depth profile

$$D(x) = D_0 x^{4/5}, \quad (2)$$

where x is the fractional distance from the head to the mouth (depth D_0).

2.3 Depth at the mouth, D_0 , and Morphological Zone

Prandle (2004a) extended these morphological theories by introducing existing expressions for saline intrusion length, L_I . By further introducing the requirement that saline mixing be contained within the estuarine length, expressions were derived for: i) the depth at the mouth D_0 in terms of river flow Q and ii) boundaries for a ‘zone of morphological existence’.

$$D_0 = 12.8 (Q a)^{0.4} \quad (3)$$

This result, shown in Figure 2, is independent of both Z and f .

$$\text{Tidal excursion: tidal intrusion} \quad E_X / L < 1, \quad (4)$$

$$\text{Saline intrusion: tidal intrusion} \quad L_I / L < 1. \quad (5)$$

The additional condition, limiting applications to ‘mixed’ estuaries is the Simpson and Hunter (1974) criterion:

$$D / U^3 > 55 \text{ (s}^3 \text{ m}^{-2}\text{)}. \quad (6)$$

These conditions are shown in Figure 3. Note: $E_X = (P_R U_T) / \pi$, where P_R is the tidal period.

3. Observational data set

The parameters available from the Future-Coast data sets include:

V_H	volume at High Water (HW)
V_L	volume at Low Water (LW)
S_H	surface area at HW
S_L	surface area at LW
Z_R	tidal range between HW and LW

- L length of tidal intrusion
 Q_{\max} maximum monthly rainfall over a 5-year period

Corresponding parameters derived for this study are:

Maximum depth $D = 0.5(V_H/S_H + V_L/S_L)$

Expanding Equation (2) for a triangular section with $D = 6.5$ m and $Z = 1.8$ m (from Table 1), the above yields 0.92 of the maximum depth at the mouth.

Mean tidal amplitude $Z = Z_R/(2 \times 1.55)$

1.55 is representative of the ratio between maximum and average tidal range, reflecting typical values for M_2 , S_2 and N_2 tidal constituents around the UK coast.

Mean flow $Q = Q_{\max}/20$

This simple approximation was based on ratios of $Q_{\text{mean}}:Q_{\text{max}}$ for major estuaries where longer term statistics exist. Mean values for residual velocity, U_0 , associated with river flow can be calculated from the values for $Q a / D^2$ shown in Table 1. Values of U_0 for estuaries of Types 1 to 4 (all estuaries, Rias, Coastal Plain and Bar Built) are 0.5, 0.04, 0.3 and 1.0 cm s^{-1} , respectively. Prandle (2004a) shows that values of U_0 derived both from observations worldwide and numerical model calculations are generally in the range 0.2 to 1.5 cm s^{-1} . The much lower values for Rias reflect their peculiar morphological development.

Mean breadth $B = (S_H + S_L)/2L$

While the derived values for D and B strictly reflect mean estuarine conditions, the tendency for both volumes and surface areas to increase significantly towards the mouth makes them sensibly representative of conditions at the mouth as required for the subsequent comparisons against theoretical expressions. It must be recognised that ‘observed’ values for D , L and B cannot be precisely determined and this ‘uncertainty’ limits the precision of subsequent comparisons against theoretical values.

4 Comparison of observations and dynamical derivations

4.1 Statistical analyses

The observational data set extends over a diverse range of estuaries. In the following assessment it should be noted that uncertainties and inaccuracies can be introduced both during the original collection and in the subsequent syntheses of these data. The only prior filtering of these data involved the application of the condition that $L > 2.5$ km. From (1), this condition corresponds to $D > Z^{0.4}$ for $Z > 1$ m (satisfying (6) as shown in Figure (3)) which might be regarded as an effective minimum value for an estuary to ‘function’ over a complete tidal cycle. All statistical fits remove two outliers – as determined by iterative calculations.

The subsequent analyses are sub-divided into four categories: i) all estuaries, ii) Rias, iii) Coastal Plain and iv) Bar Built. The numbers, N , in each category are: 80(28), 15(61), 30(45) and 35(42) with the bracketed figures indicating percentage significant correlation at the 99% level.

An estimate of percentage of variance accounted for (PVA), is used where

$$\text{PVA} = 100 \times \{1 - (\sum |O_i^2 - C_i^2|) / \sum O_i^2\} \quad (7)$$

with O_i observed and C_i the ‘best’ statistical fit over summations $i = 1$ to N . The use of normalised PVA is appropriate for the large parameter ranges involved. The statistical fit is assumed to take the form $A y^P$, with A calculated from least squares over the range $-3 < P < 3$ (in increments of 0.01) and with P chosen to reflect the maximum value for PVA. The numerical optimisation calculates r^{-q} versus s^q , where r and s are any fitted parameter, and $q = P^{1/2}$ so that the fit applies when the order of the parameters is reversed.

Attempts were made to extend the statistical fits to multiple parameters. The results were less conclusive and did not usefully expand the above approach.

4.2 The range of estuarine parameters: mean, minimum and maximum values

The data in Table 1 usefully quantify the descriptions of estuarine types outlined by Davidson and Buck (1997). Thus, in general, Rias are short, deep and steep-sided with small river flows. Coastal Plain estuaries are long and funnel-shaped with gently sloping triangular cross-sections providing extensive inter-tidal zones. Bar Built estuaries are short and shallow

with small river flows and tidal range. As noted in Section 3.1, sandy estuaries tend to be short and muddy estuaries tend to be long.

In sedimentary terms, Bar Built estuaries are located along coasts with plentiful supplies of marine sediments and, consequently, are close to present-day equilibrium. Coastal Plain estuaries are continuing to infill following ‘over-deepening’ via post-glacial river flows while Rias are drowned river valleys (with related cross-sections) as a consequence of (relative) sea level rise.

The mean side-slope gradient, $a = 0.013$, corresponds to a maximum lateral velocity, $2\pi Z / (a P_R)$, of about 2 cm s^{-1} .

Further to the earlier discussion (Section 4.1) of the minimum depth of an estuary is the issue of the minimum river flow, Q , required to maintain a continuous dynamical link to the sea. Ian Townend (personal communication, 2005) found from model studies that a flow of $0.25 \text{ m}^3 \text{ s}^{-1}$ was necessary to prevent sedimentation of tidal creeks. Applying the criteria that $D > Z^{0.4}$ establishes a minimum depth for estuarine functioning. Substituting the values for transverse slope, a , from Table 1 into Equation (3) we derive minimum values of Q ($\text{m}^3 \text{ s}^{-1}$) for $Z = 1, 2$ and 4 m of:

- i) all estuaries 0.13, 0.75, 4.2;
- ii) Rias 0.05, 0.26, 1.5;
- iii) Coastal Plain 0.15, 0.88, 5.0;
- iv) Bar Built 0.12, 0.69, 3.9.

4.3 Spacing between estuaries

Assuming a rectangular catchment of landward extent C (km) and river flow, Q , the spacing, S (km), between estuaries can be calculated as:

$$S = 31 Q / CR, \tag{8}$$

where R (m a^{-1}) is the annual rainfall reaching the river. Thus $R \approx 0.9 \text{ m a}^{-1}$ for typical UK values of $S = 10$ km, $C = 50$ km, $Q = 15 \text{ m}^3 \text{ s}^{-1}$. By introducing Equation (3) with $a = 0.013$ from Table 1, we obtain:

$$S = 41 D^{5/2} / CR. \quad (9)$$

We note from Table 1 and from global observational data shown by Prandle (2004a) that few estuaries have values of $D > 20$ m. Hence to avoid small values of S for Continental land masses with large values of C , we might anticipate the formation of Deltas or multiple ‘sub-estuaries’ linked to the sea by tidal basins such as in Chesapeake Bay.

4.4 Estuarine Morphology

The relationships between L and D , shown in Table 2, are consistent and are in good agreement with theory. The relationships between B and D show much greater scatter. Alongside the range of values for ‘ a ’ shown in Table 1, this result emphasises the likely diversity in inter-tidal ecosystems between estuarine types. The latter result is further reflected in the wide spread in the relationships between B and L .

Prandle and Rahman (1980) introduced a parameter, v , to represent the dynamical influence of funnelling, this corresponds to

$$v = \frac{n+1}{2-m}, \quad \text{where } B(x) \propto x^n \quad \text{and} \quad D(x) \propto x^m. \quad (10)$$

Taking the powers of L (in B versus L) to reflect n and the inverse of the power of D (in L versus D) to reflect m , the corresponding values of v are shown in Table 2. Maximum tidal amplification occurs for $v \approx 1$ with considerable reduction of this peak for $v = 2$. Thus tidal elevations and currents are likely to be more spatially homogeneous in Bar Built estuaries reflecting conditions closer to equilibrium.

The estuarine length, L_M , for maximum amplification is approximated by:

$$L_M = (2-m)(0.75v + 1.25)g^{1/2}D^{1/2}P_R / (4\pi). \quad (11)$$

Substituting $m = 0.8$ and $v = 2.0$ gives $L_M = 37 D^{1/2}$ (km) or 94 km for $D = 6.5$ m. This indicates that only the longest of UK estuaries, such as the Bristol Channel, are likely to exhibit significant tidal amplification.

Figure 1 shows the relationships between L and $D^{1.25}/Z^{1/2}$ from Equation (1), including the likely range between sandy and muddy estuaries. Corresponding coordinates for the observational data determined in Section 3 are plotted (and equivalently in Figures 2 and 3). The statistical relationships between observed values of L and D , indicated in the first column of Table 2, are also shown. The wide spread of observational data for Coastal Plain estuaries reflects their stages of morphological adjustment. However, the plotted statistical fits for both Coastal Plain and Bar Built estuaries lie close to the plot for (1). The power, 1.10, of D for Rias is in reasonable agreement with the theoretical value of 1.25 but the reduced value of the coefficient A reflects the shorter lengths of these estuaries.

Overall we note statistically significant relationships between all of these estuarine parameters in all types of estuaries – indicating the tendency for estuarine morphologies to be confined within restricted parameter ranges

4.5 Relationships between estuarine morphology and external forcing tidal amplitude Z and river flow Q

Table 3(a) shows, from observed bathymetries of Coastal Plain estuaries, that on average $B \sim Z^{2.87}$ and $D \sim Z^{2.00}$ indicating that the side-slope $a \sim Z^{-0.87}$. Hence we expect a decrease in ‘ a ’ towards the mouth (larger Z), resulting in increased plan-form funnelling compared with Equation (2).

Table 3(a) indicates a high correlation between depth D and tidal amplitude Z . This result counters the implication from (1) that, if Z and D were independent of each other, tidal lengths would increase for smaller tidal amplitudes.

Figure 2 shows the theoretical result, (3), with $a = 0.013$ from Table 1. As in Figure 1, the Coastal Plain estuaries show widely scattered points. However the statistical fits, from Table 3(b), are in reasonable agreement with the theory with powers of Q of 0.31 for Rias and 0.38 for both Coastal Plain and Bar Built estuaries close to the theoretical value of 0.4. Moreover the related values for the coefficient ‘ A ’ result in distributions close to the theory although with enhanced depths for Rias.

Figure 3 shows the ‘morphological existence zone’ bounded by Equations (4), (5) and (6). These encompass most of the observed estuaries. From column 1 of Table 3a, the

observational fits indicate $Z \propto D^{0.5}$ for Coastal Plain estuaries and $Z \propto D^{0.65}$ for Bar Built. For $Z < 3$ m, the statistical fits closely bisect the theoretical zone. For $Z > 3$ m, Prandle (2004a) shows that tidal current amplitudes exceed 1.5 m s^{-1} and the axial slope of the bed increases significantly. Consequently, such estuaries are generally in the form of deep contiguous bay-estuary systems such as the Bristol Channel or Bay of Fundy.

5. Summary and conclusions

This study uses recently compiled data from 80 UK estuaries to assess new dynamically-based theories of estuarine bathymetry. While individual estuaries exhibit localised features (related to underlying geology, flora and fauna, historical development and ‘intervention’) the overall values of depth, length and (funnelling) shape were shown to be consistent with the new dynamical theories. Moreover, the morphological features which characterise Rias, Coastal Plain and Bar Built estuaries can be rationalised by reference to these theories.

Size

Length, L : the theoretical dependency of L on $D^{1.25}$ was substantiated for all three estuarine types. Despite a wide scatter, particularly for Coastal Plain estuaries, the statistical fit suggests values of L in close agreement with the theory for both Coastal Plain and Bar Built estuaries; the fit for Rias indicates significantly reduced values for L .

Depth, D : the theoretical dependency of D on $Q^{0.4}$ was similarly substantiated for all three estuarine types. The statistical fits also provided close quantitative agreement for Coastal Plain and Bar Built estuaries while that for Rias indicated significantly larger values of D .

Shape

The theory indicates D varying with $x^{0.8}$ (x is the fractional distance from the head). This translates into increasingly funnelling plan forms for Rias to Coastal Plain to Bar Built estuaries via a reduction in cross-shore slopes between the head and mouths of estuaries. The mean dynamical funnelling rate, encapsulated by $v \approx 2$ (Prandle and Rahman, 1980), suggests that most UK estuaries will not show significant tidal amplification. Classical quarter-wavelength resonance will be confined to the largest of estuaries with values of $D > 90$ km.

Limiting dimensions

Minimum values of $D \geq Z^{0.4}$ and of the order $Q \geq 0.25 \text{ m}^3 \text{ s}^{-1}$ are required for estuarine functioning over the complete tidal cycle. Typical maximum values of around $D \leq 20$ m and

$Z \leq 3$ m can be postulated and used to suggest the formation of deltas and composite estuaries in draining large Continental land masses.

Year 2100 morphologies – impacts of changes in mean sea level and river flows

The agreement between theory and observations noted above provides encouragement for estimating future morphological changes resulting from changes in mean sea level and river flows associated with Global Climate Change. Estimates of ‘precautionary’ (plausible values appropriate for scenario testing) changes in sea level involve an increase of 50 cm by 2100 and for river flow both increases and decreases of up to 25% (Defra/Environment Agency Technical Summaries, 2003 and 2004).

By inserting these changes in river flow, Q , in Equation (3) and the resulting changes in depth, D , into (1) we can estimate the changes in length, L . Likewise the changes to breadth, B , associated with the changes in D can be estimated by assuming the side-slope gradients, a , shown in Table 1 are unchanged. Table 4 shows these resultant changes. The changes, δD , in D correspond to $\delta Q^{0.4}$, changes in L to $(\delta Q^{0.4})^{1.25}$ and in B to $2 \delta D / a$.

The results show that, on average, the ‘dynamical’ adjustment to a 25% change in river flows may change depths as much as the projected sea level rise – with this effect reduced in smaller estuaries and significantly increased in larger ones. The resulting changes in estuarine lengths and breadths follow similar patterns with the biggest ‘dynamical’ change occurring in the largest estuaries where they are significantly greater than those due to sea level rise.

Overall we anticipate changes in: estuarine lengths of the Order (0.5 to 5 km) and breadths of Order (50 to 250 m) due to the 25% change in river flow. Corresponding changes due to a sea level rise of 50 cm are increases in both lengths of Order (1 to 2.5 km) and breadths of Order (70 to 100 m).

The dynamical theories do not consider the sediment regimes in estuaries, these processes need to be introduced to quantify the related time scales for morphological adjustment (Prandle, 2004b).

Further Studies

An objective assessment has been presented of the applicability of new theories which relate estuarine bathymetries to: i) tidal dynamics, encapsulated by the mean tidal amplitude at the mouth, Z , and ii) the average river flow, Q . The principle outcomes are expressions for estuarine length, depth and axial profile as functions of the ‘forcing’ parameters Z and Q . A consequent paradigm shift suggests that prevailing sediment regimes are the consequence of rather the determinant for these bathymetries. The frameworks shown here provide perspectives against which to assess the morphology of any particular estuary. Furthermore, ‘anomalous’ estuaries can be identified, and related causal mechanisms explored.

A specific objective of this paper was to provide insight into the applicability of these expressions and thence stimulate refinements. This will require extending the present assessment to encompass detailed local knowledge of specific estuaries, allowing for impacts of: engineering ‘interventions’, ‘hard’ geology, dynamics or mixing inconsistent with the theoretical assumptions, non-representative observational data, vagaries of sediment supply, wave impact, etc. Studies of regional patterns of historical estuarine evolution should provide insight into the impacts of these various factors described above and, thereby, help refine the new expressions.

A further factor concerns the impact of flora and fauna that have long been recognised as influencing the supply, consolidation and turbation of bed sediments. Prandle (2004b) showed how variations in the effective bed friction factor, f , have a major impact on dynamics and thence on both morphology and the sediment regime. It is this latter aspect of flora and fauna that may be most significant. Indeed, if long-term bathymetric evolution cannot be predicted by extrapolation of prevailing net scour or erosion, scenarios based on combinations of (climatic) perturbations to the controlling parameters of (Z , Q), alongside variations in f due to related changes in flora and fauna might be explored. Such scenarios might include relatively rapid and discontinuous changes following ‘extreme’ events.

Acknowledgements

This study was supported by Research Project FD2107 – Development of Morphological Models. The Project forms Part 2 of the UK Estuaries Research Programme funded by the Broad Scale Modelling Theme within Defra/Environment Agency’s Flood Management Research Programme.

References

- Burgess, K.A., Balson, P., Dyer, K.R., Orford, J., Townend, I.H., 2002. Future-Coast – The integration of knowledge to assess future coastal evolution at a national scale. pp3221–3233 in: 28th International Conference on Coastal Engineering. Am. Soc. of Civ. Eng., Cardiff, UK.
- Davidson, N.C., Buck, A.L., 1997. An inventory of UK Estuaries Volume 1 (of 7) ‘Introduction and Methodology’. 46pp. Published by Joint Nature Conservation Committee, Peterborough, UK.
- Defra/Environment Agency, 2003. Climate change scenarios UKCIP02: Implementation for flood and coastal defence. R&D Technical Summary W5B-029/TS.
- Defra/Environment Agency, 2004. Impact of climate change on flood flows in river catchments. Technical Summary W5-032/TS.
- Lane, A., 2004. Bathymetric evolution of the Mersey Estuary, UK, 1906–1997: cause and effect. *Estuarine, Coastal and Shelf Science*, 59, 249–263, doi:10.1016/j.ecss.2003.09.003.
- Lane, A., Prandle, D., 2006. Random-walk particle modelling for estimating bathymetric evolution of an estuary. To appear in *Estuarine, Coastal and Shelf Science*.
- Prandle, D., Rahman, M., 1980. Tidal Response in Estuaries. *Journal Physical Oceanography*, 10(10), 1552–1573, doi: 10.1175/1520-0485(1980)010<1552:TRIE>2.0.CO;2.
- Prandle, D., 2003. Relationships between tidal dynamics and bathymetry in strongly convergent estuaries. *Journal of Physical Oceanography*, 33(12), 2738–2750, doi: 10.1175/1520-0485(2003)033<2738:RBTDAB>2.0.CO;2.
- Prandle, D., 2004a. How tides and river flows determine estuarine bathymetries. *Progress in Oceanography*, 61, 1–26, doi:10.1016/j.pocean.2004.03.001.
- Prandle, D., 2004b. Sediment trapping, turbidity maxima, and bathymetric stability in macrotidal estuaries. *Journal of Geophysical Research*, 109, C08001, 13pp, doi:10.1029/2004JC002271.
- Prandle, D., Lane, A., Manning, A.J., 2005. Estuaries are not so unique. *Geophysical Research Letters*, 32, L23614, doi: 10.1029/2005GL024797.
- Simpson, J.H., Hunter, J.R., 1974. Fronts in the Irish Sea. *Nature*, 250, 404–406.
- Woodroffe, C.D., 2003. *Coasts: form, process and evolution*. Cambridge University Press, 623pp.

Tables

Table 1: Mean values of Z , Q , D , L , B and ' a ' for four estuarine types.

		Minimum (10th percentile) and maximum (90th percentile) values for Type 1					
Type		Z (m)	Q ($\text{m}^3 \text{s}^{-1}$)	D (m)	L (km)	B (m)	a
1	All	1.80	14.9	6.5	20	970	0.013
	Minimum	1.20	0.2	2.5	5	130	0.004
	Maximum	2.60	35.9	17.3	41	3800	0.129
2	Ria	1.70	6.3	9.3	12	490	0.037
3	Coastal Plain	2.00	17.9	8.1	33	1500	0.011
4	Bar Built	1.61	9.5	3.6	9	510	0.014

Table 2: Statistical fits between B , L and D .

L in km, D and B in m, figures in brackets indicate PVA.

**Equation (1) for $f = 0.0025$ and $Z = 1.8$ m.

Type	$L \sim A D^P$	$B \sim A D^P$	$B \sim A L^P$	$v = (n + 1)/(2 - m)$
1 All	$1.28 D^{1.24}$ (69)	$38 D^{1.38}$ (59)	$15.7 L^{1.20}$ (69)	1.85
2 Ria	$0.99 D^{1.10}$ (89)	$25 D^{1.33}$ (95)	$51.4 L^{0.89}$ (94)	1.72
3 Coastal Plain	$1.95 D^{1.12}$ (69)	$93 D^{1.10}$ (64)	$7.8 L^{1.30}$ (64)	2.07
4 Bar Built	$1.92 D^{1.15}$ (66)	$25 D^{1.99}$ (66)	$9.4 L^{1.55}$ (71)	2.25
Theory**	$1.83 D^{1.25}$			

Table 3a: Statistical fits between D , L and B with Z

Type	$D \sim A Z^P$	$L \sim A Z^P$	$B \sim A Z^P$
1 All	$1.3 Z^{2.47}$ (78)	$5.1 Z^{1.27}$ (57)	—
2 Ria	—	—	—
3 Coastal Plain	$1.7 Z^{2.00}$ (82)	$4.3 Z^{2.55}$ (78)	$139 Z^{2.87}$ (76)
4 Bar Built	$2.0 Z^{1.58}$ (80)	$7.4 Z^{1.44}$ (45)	—

Blank indicates no minimal value (best fit) found within the range of powers $-3 < P < 3$.

Table 3b: Statistical fits between D , L and B with Q

**Equation (3) with $a = 0.013$ from Table 1

Type	$D \sim A Q^P$	$L \sim A Q^P$	$B \sim A Q^P$
1 All	$3.3 Q^{0.47}$ (55)	$3.0 Q^{0.68}$ (64)	$98 Q^{0.86}$ (75)
2 Ria	$5.1 Q^{0.31}$ (74)	$3.1 Q^{0.74}$ (93)	$41 Q^{1.05}$ (80)
3 Coastal Plain	$3.0 Q^{0.38}$ (67)	$6.7 Q^{0.64}$ (89)	$106 Q^{0.85}$ (71)
4 Bar Built	$2.4 Q^{0.38}$ (72)	$9.2 Q^{1.37}$ (21)	$11 Q^{1.37}$ (50)
Theory**	$2.3 Q^{0.4}$		

Table 4 Changes in depth D , length L and breadth B due to:

25% change in river flow subscript ' Q ',
 0.5 m increase in mean sea level subscript ' msl '.

Estuary type	D (m)	δD_Q	L (km)	δL_Q	δL_{msl}	B (m)	δB_Q	δB_{msl}
		+ / -		+ / -	+		+ / -	+
All min	2.5	0.25	5	0.62	1.28	130	38	}
All mean	6.5	0.65	20	2.50	1.94	970	100	} 77
All max	17.3	1.73	41	5.12	1.49	3800	266	}
Coastal Plain	8.1	0.81	33	4.12	2.57	1500	147	91
Bar Built	3.6	0.36	9	1.12	1.59	510	51	71

List of Figures

Figure 1: **Tidal intrusion length, L ,** $L = 123 D^{5/4} / (fZ)^{1/2}$ continuous lines
 $f = 0.0025$ thick line, $f = 0.005$ and $f = 0.00125$ thin lines,
 D depth and Z tidal elevation at the mouth, f friction factor.

Statistical fits to observations: Ria $L = 0.99 D^{1.10}$ dashed
 Coastal Plain $L = 1.95 D^{1.12}$ dot-dash
 Bar Built $L = 1.92 D^{1.15}$ dotted

Figure 2: **Depth at the mouth, D ,** $D = 12.8 (aQ)^{0.4}$ continuous line
 ‘ a ’ transverse slope (0.016), Q river flow

Statistical fits to observations: Ria $D = 5.1 Q^{0.31}$ dashed
 Coastal Plain $D = 3.0 Q^{0.38}$ dot-dash
 Bar Built $D = 2.4 Q^{0.38}$ dotted

Figure 3: **Morphological Zone,** Tidal elevation amplitude, Z , versus depth, D ,
 bounded by: continuous lines

$E_X / L = 1$ left
 $L_I / L = 1$ right
 $D / \hat{U}^3 = 55 \text{ m}^{-2} \text{ s}^3$ bottom

E_X , tidal excursion length; L_I , salinity intrusion length, L estuary length,
 D / \hat{U}^3 Simpson and Hunter (1974) mixing parameter.

Statistical fits to observations: Coastal Plain $Z = 0.77 D^{0.50}$ dot-dash
 Bar Built $Z = 0.64 D^{0.63}$ dotted

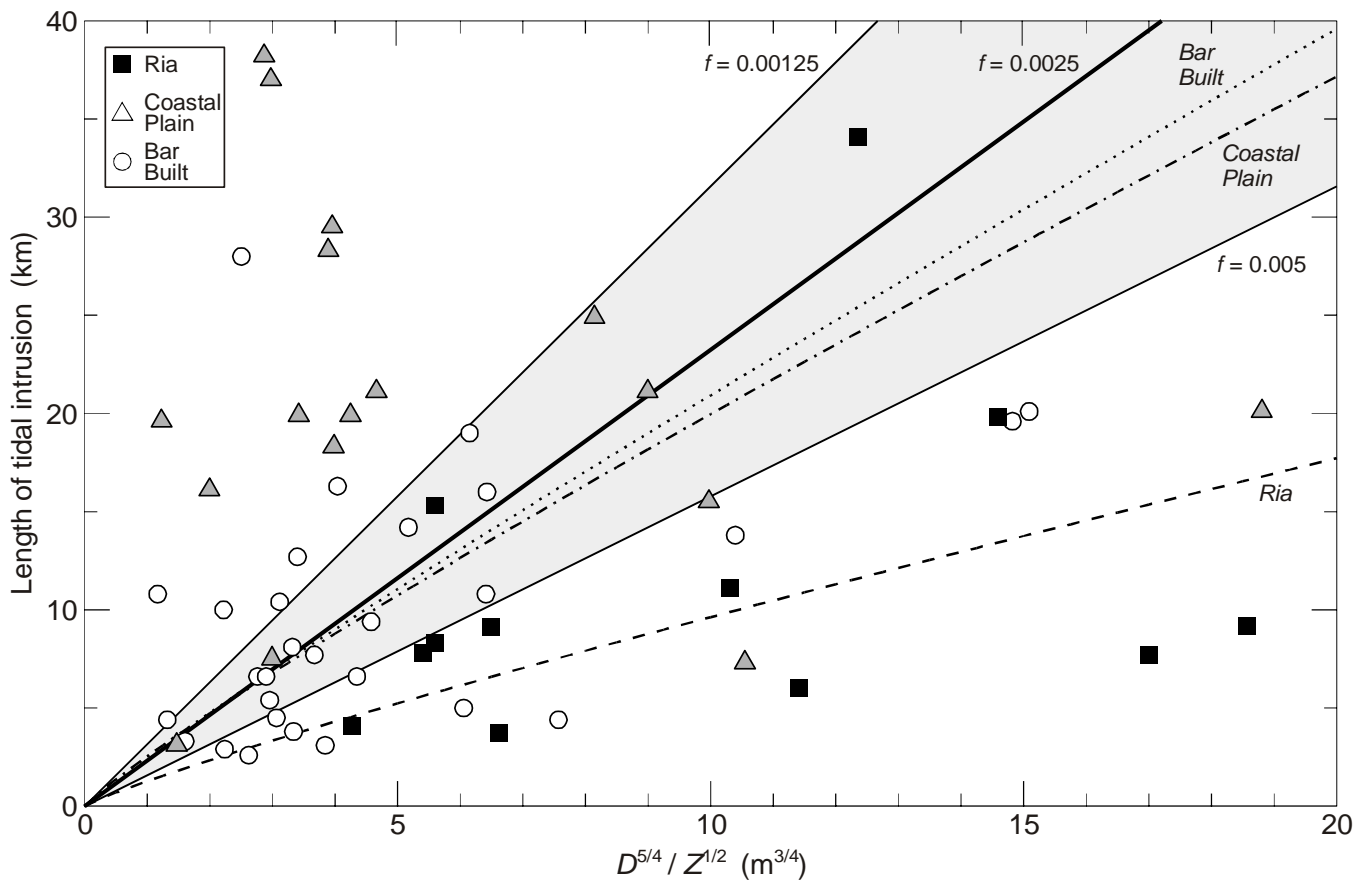


Figure 1: **Tidal intrusion length, L ,** $L = 123 D^{5/4} / (fZ)^{1/2}$ continuous lines
 $f = 0.0025$ thick line, $f = 0.005$ and $f = 0.00125$ thin lines,
 D depth and Z tidal elevation at the mouth, f friction factor.
 Statistical fits to observations: Ria $L = 0.99 D^{1.10}$ dashed
 Coastal Plain $L = 1.95 D^{1.12}$ dot-dash
 Bar Built $L = 1.92 D^{1.15}$ dotted

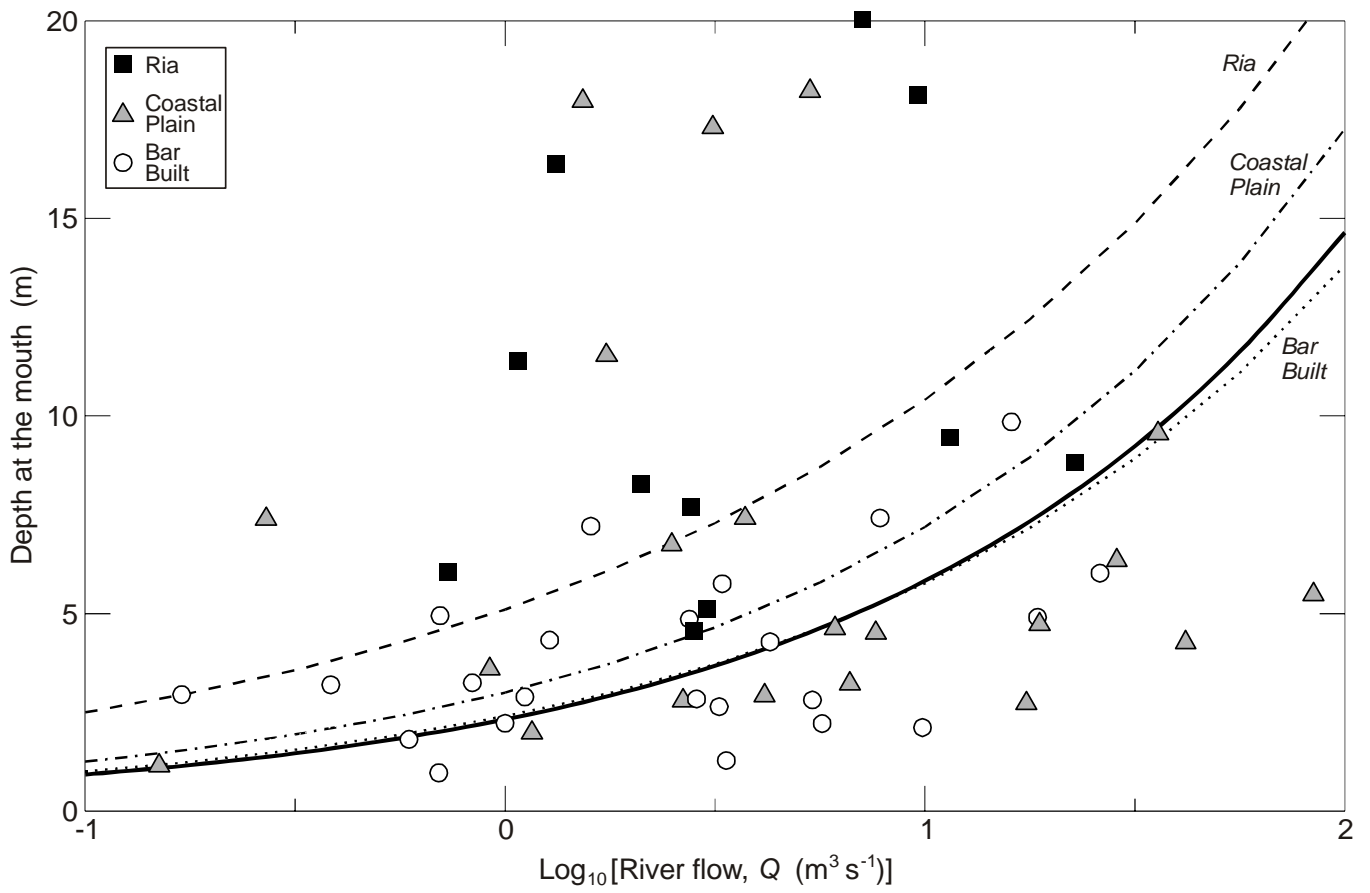


Figure 2: **Depth at the mouth, D ,** $D = 12.8 (a Q)^{0.4}$ continuous line
 'a' transverse slope (0.016), Q river flow
 Statistical fits to observations:

Ria	$D = 5.1 Q^{0.31}$	dashed
Coastal Plain	$D = 3.0 Q^{0.38}$	dot-dash
Bar Built	$D = 2.4 Q^{0.38}$	dotted

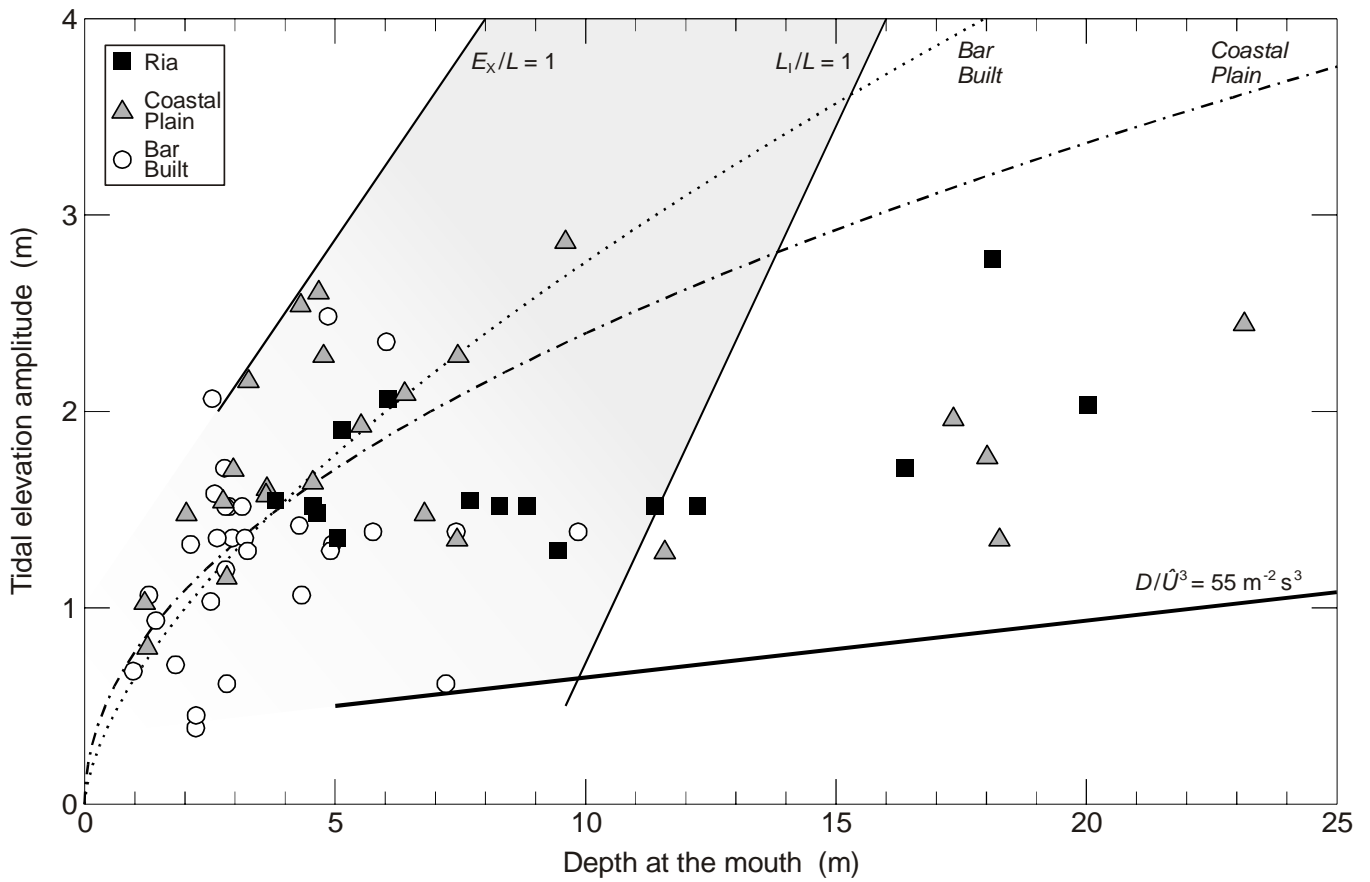


Figure 3: **Morphological Zone**, Tidal elevation amplitude, Z , versus depth, D ,
 bounded by: continuous lines

$E_x / L = 1$ left
 $L_1 / L = 1$ right
 $D / \hat{U}^3 = 55 \text{ m}^{-2} \text{ s}^3$ bottom

E_x , tidal excursion length; L_1 , salinity intrusion length, L estuary length,
 D / \hat{U}^3 Simpson and Hunter (1974) mixing parameter.

Statistical fits to observations: Coastal Plain $Z = 0.77 D^{0.50}$ dot-dash
 Bar Built $Z = 0.64 D^{0.63}$ dotted